

Contents lists available at ScienceDirect

Carbon Trends

journal homepage: www.elsevier.com/locate/cartre



Check for updates

Effect of carbonization methods on graphitization of soft and hard carbons

Sandra Ike a,b,*, Randy Vander Wal a,b

- ^a The John and Willie Leone Family Department of Energy and Mineral Engineering Penn State University 16801, USA
- ^b EMS Energy Institute, Penn State University 16801, USA

ARTICLE INFO

Keywords:
Autogenic pressure
Atmospheric pressure
Graphitization
Resole
PVC

ABSTRACT

Pressurized carbonization is known to improve carbon content and create textural changes in resultant carbon compared to conventional (atmospheric) carbonization. However, further studies investigating the impact of these carbonization methods on the graphitic quality of the carbon precursors have not been explored extensively. This study investigates the influence of carbonization methods on the graphitization behavior of soft and hard carbons using a three-model system: phenolic resole (hard carbon), polyvinyl chloride (PVC) (soft carbon), and a 50:50 blend of resole and PVC. Carbonization was conducted under autogenic pressure (AGP) and atmospheric pressure (APP) at 500 °C for 5 h, followed by high-temperature treatment at varying temperatures. Various techniques, including X-ray diffraction and Raman spectroscopy showed hard carbon precursors exhibited improved properties under AGP carbonization such as larger crystallite size, sharp crystalline peaks, lower I_D/I_G ratio, and narrow G-full width half-maximum, an indication of improved crystallinity by lowering amorphous phase at high temperature. For soft carbon precursors, the method of carbonization did not impact the graphitization level. The most significant finding was the enhanced crystalline nature observed in hard carbon under AGP conditions, without the need for any catalyst. It shows the influence of pressure on improving the crystallinity of hard carbon precursors.

1. Introduction

Carbonization is the process of concentrating and purifying carbon by denaturing organic matter with heat in the presence of little to no oxygen [1]. Carbonization can be classified into two regimes: atmospheric and pressurized. The atmospheric method involves heating the sample in an open boat or vessel placed in a furnace. The sample is typically heated at a slow heating rate (0.1 °C/m to 2 °C/min) to temperatures between 500 $^{\circ}\text{C}$ - 1000 $^{\circ}\text{C},$ and a long residence time ranging from 0.5 h to 24 h or more [1,2]. During carbonization, various reactions such as deoxygenation, dehydrogenation, and dealkylation occur as the carbon precursor decomposes resulting in the evolution of hydrocarbons (short aliphatic chains) and volatile gases such as CO and CO_2 [3,4]. The release of these hydrocarbons and volatile gases leads to a lower carbon yield content of the carbonized product [5,6]. Carbonization performed under pressure is an attempt to increase the carbon yield in comparison to atmospheric carbonization [7-9]. Under pressure, the evolution of hydrocarbons and volatiles is suppressed which may lead to an increase in the carbonization yield [5,10].

Pressurized carbonization is typically carried out in different ways:

(1) carbonization under pressure built up by the decomposition gases of the precursor (autogenic) which stands in contrast to (2) carbonization under constant pressure, and (3) carbonization under hydrothermal conditions [5]. Carbonization under autogenic pressure is done by heating the carbon precursor from ambient to carbonization temperature with gradual pressure increase from decomposition gas built up in a closed vessel. Under autogenic conditions, pressure cannot be kept constant; it is strongly dependent on the temperature and the amount of sample used [5]. Conversely, pressure can be kept constant by using an autoclave during carbonization heat treatment.

Hydrothermal carbonization can be done at temperatures either above 400 °C, below 250 °C, or within these limits. The pressure is built up by water vapor and depends on the amount of water and volume of autoclave used [5,11]. A consequence of carbonizing under pressure is that it may change the carbonization process (gas solubility, mesophase viscosity, carbonaceous intermediates, carbon yield, etc.) which can in turn lead to the resulting carbon being different in structure, property, and even particle morphology from that obtained without pressure [5,12]. This makes pressurized carbonization a possible method for controlling the structure and texture of resultant carbons. Michio Inagaki

E-mail address: sxi5097@psu.edu (S. Ike).

^{*} Corresponding author.

et al., [5] stated that the principal purposes for carbonization under pressure include modification of carbonization behavior, improving the carbon yield, densifying the resultant carbon, changing graphitization behavior, or obtaining specific particle morphology of the resultant carbons.

There have been many studies on the effect of carbonization methods on the carbon content of precursors. Hosomura et al., [13] studied the effect of pressure carbonization on carbon-carbon (C-C) composites and conventional materials such as phenolic resins and pitches. They found that pressure carbonization does not affect the carbon yield of the hard carbons (phenolic resin and furfuryl alcohol); the carbon yield obtained was 55 % irrespective of pressure. However, there was a significant increase in the carbon yield for pitches (of low molecular weight) carbonized under pressure. Texture changes were also observed wherein the pressure carbonization increased the proportion of fine mosaic relative to coarse texture as seen by polarized light microscopy (PLM). Another study by Ayache et al., [12] also observed a change in the texture of the resultant carbon after the carbonization of polyethylene and anthracene at 650 °C under a pressure of 30 MPa. Characterizations from scanning electron microscopy (SEM), transmission electron microscopy (TEM), and optical microscopy showed that both materials had radial texture phases after pressure carbonization. Inagki et al., [14] carbonized coal tar pitches at 650 °C under a pressure of 30 MPa in closed and open gold tubes. The carbon yield of the original pitch was 96 % and 51 % under the closed and open systems respectively. The low carbon yield in the open system was attributed to hydrocarbons and volatiles lost during carbonization whereas in the closed system, the decomposition gases react with the mesophase, increasing the high carbon content to greater than 90 %.

Despite these findings, however, there are comparatively few studies of carbonization pressure effects on the graphitization behavior and final (graphitic quality) of the final carbon product. In one such study, Kamiya et al., [15] graphitized three polyvinyl alcohol (PVC) samples under normal pressure after preheating (at 1470 $^{\circ}$ C, 1590 $^{\circ}$ C, and 1620 $^{\circ}$ C) under pressure of 5 kbar. These authors found that the treatment of soft carbon under high pressure had no accelerating effect on the carbon graphitization in the subsequent heat treatment under normal pressure.

This study, however, does not specifically examine hard carbons which would be a useful contribution to understanding if pressure carbonization can influence graphitization behavior. Okamoto et al., studied the effect of pressure on carbonization and subsequent graphitization on phenolic resins [16]. Phenolic resins were carbonized at 650 °C under atmospheric or 100 MPa pressures and iron oxide was used as a catalyst. Subsequent heat treatments were conducted at 1200 °C, 1500 °C, and 1900 °C. The study measured carbon yield, density, and crystallinity as well as optical observations. Results indicated that pressurized carbonization of phenolic resin advanced graphite crystallization accelerated by iron oxide powder. This study's focus was on the catalyst effect and the sole effect of pressure during carbonization was not discussed. This therefore highlights the need for a rigorous fundamental study on the effect of pressure on non-graphitizing carbons. Moreover, understanding the graphitization of hard carbons is on the uprise and has become a hot topic in the scientific community [17-19] and industry as the precursor to synthetic graphite due to its abundance and environmental friendliness.

In this work, we selected two precursors non-graphitizing (hard carbon, resole), graphitization (soft carbon, polyvinyl alcohol (PVC)), and their blend (50:50 by weight) to study the effect of carbonization methods on graphitization. During carbonization, we subjected the samples to atmospheric and autogenic pressure carbonization and subsequent high-temperature heat treatment. Detailed analysis from X-ray diffraction (XRD), Raman spectroscopy, transmission electron microscope (TEM), and selected area diffraction (SAED) showed a trend of improved graphitic quality in the form of larger crystallite size (La), sharp crystalline peak, lower $\rm I_D/I_G$ ratio, narrow G-full width half-maximum for the non-graphitizing precursors because of pressurized

carbonization. For the graphitizing or soft carbon precursor pressure carbonization does not show any change in graphitization level. The improved crystalline nature in hard carbon under pressure without the addition of any catalyst is an important finding.

2. Experimental sections

2.1. Materials

Polyvinyl chloride (PVC – molecular weight of 62,000) was used as received from Sigma Aldrich without any further modification. The resin used was a resole from Supelco (Plenko 14,946 resole). Material preparations included the resole, PVC, and a blend (50/50 resole+PVC) of each. Samples were placed in an oven at 100 $^{\circ}\text{C}$ for 24 h to remove moisture.

2.1.1. Carbonization

The three samples (PVC, resole, and resole + PVC) were carbonized by two methods: atmospheric and autogenic pressure. Carbonization under atmospheric pressure (APP) was done in an open boat in a Thermolyne 2110 tube furnace with a heating rate of 2 °C/min, while carbonization under autogenic pressure (AGP) was performed in a customized pressurized reactor. For AGP, the sample was wrapped in brass foil and inserted into the reactor, which was then pressurized with nitrogen to purge all oxygen out and checked for leaks. The pressure in the reactor typically ranged between 500 - 1000 psi during the carbonization process. The heating rate, cooling conditions, and temperature control specifics were maintained to ensure consistent results. Carbonization by both methods was conducted at 500 °C for 5 h. The reactor's pressure control precision and heating rates were carefully monitored to maintain consistent conditions throughout the process.

2.1.2. Graphitization

The conventional and pressure-carbonized samples (six samples in total) were graphitized at three different temperatures: $1000\,^{\circ}\text{C}$, $1500\,^{\circ}\text{C}$, and $2500\,^{\circ}\text{C}$. The $1000\,^{\circ}\text{C}$ graphitization was carried out in a Thermolyne 2110 tube furnace at a heating rate of $15\,^{\circ}\text{C}/\text{minute}$. The $1500\,^{\circ}\text{C}$ graphitization was performed in a GSL-1700X-UL furnace with a temperature ramp-up at a rate of $10\,^{\circ}\text{C}/\text{min}$ to $900\,^{\circ}\text{C}$ and then at $5\,^{\circ}\text{C}/\text{min}$ to $1500\,^{\circ}\text{C}$. Graphitization at $2500\,^{\circ}\text{C}$ was done in a Centorr Vacuum Industries series 45 graphitization furnace, heating at $15\,^{\circ}\text{C}/\text{min}$ to $1000\,^{\circ}\text{C}$, $10\,^{\circ}\text{C}/\text{min}$ to $2000\,^{\circ}\text{C}$, and finally at $5\,^{\circ}\text{C}/\text{min}$ to $2500\,^{\circ}\text{C}$. All graphitization processes were carried out under an inert atmosphere to prevent oxidation and ensure consistent material properties.

2.2. Characterizations

2.2.1. Thermogravimetric analysis (TGA)

Thermogravimetric analysis (TGA) was done in a Q600 (TA Instruments, USA). Pre-carbonized samples were subjected to a temperature ramp test (30 - 900 $^{\circ}\text{C}$ at 10 $^{\circ}\text{C/min}$). The conventional and pressure carbonized samples were subjected to the same temperature ramp test, however, with an isothermal hold at 900 $^{\circ}\text{C}$ for 120 min to study the carbon content of each sample.

2.2.2. X-ray diffraction (XRD)

The X-ray diffraction patterns were collected using a Malvern PAN-alytical Empyrean diffractometer equipped with Cu source ($\lambda\cong 1.54 A^\circ$), para-focusing optics, and PIXcel 3D detector. The spectrum was scanned in the 2θ range from 10° to 90° The background subtraction, peak fitting, and quantification were done using MDI JADE® software.

2.2.3. Raman spectroscopy

Raman spectra were collected using a Horiba LabRAM HR Evolution equipped with a 300 groove/mm grating and a 532 nm laser. The spectra were acquired in DuoScan $^{\rm TM}$ mode which increases the statistical

significance of the data by rastering over a wider area. At least 5 measurements were collected for each sample to ensure the analysis was representative.

2.2.4. Transmission electron microscope (TEM) and selected area electron diffraction (SAED)

Transmission electron microscope samples were prepared by sonicating a few milligrams (mg) of graphitized material in ethanol and then a droplet of the suspension was placed on a copper (Cu) supported lacey carbon grid and allowed to dry. The samples were imaged using a FEI TalosTM F200X scanning/transmission electron microscope equipped with an FEG source providing 0.12 nm resolution. The instrument was operated at 200 kV and the samples were imaged at various magnifications in the ranges. Selected area electron diffraction (SAED) patterns were taken concurrently with TEM imaging.

2.2.5. Scanning electron microscope (SEM)

SEM images were taken with field-emission SEM: Apreo. Samples were prepared by placing a few milligrams on a carbon-taped pin stub holder. To obtain FESEM images, an acceleration voltage of 7 kV and a working distance between 11 mm to 7 mm were maintained.

2.2.6. X-ray photoelectron spectroscopy (XPS)

XPS experiments were performed using a Physical Electronics VersaProbe II instrument equipped with a monochromatic Al K_{α} X-ray source (h $\nu=1486.7$ eV) and a concentric hemispherical analyzer.

Charge neutralization was performed using both low energy electrons (<5 eV) and argon ions. The binding energy axis was calibrated using sputter cleaned Cu (Cu $2p_{3/2}=932.62$ eV, Cu $3p_{3/2}=75.1$ eV) and Au foils (Au $4f_{7/2}=83.96$ eV). Peaks were charged with reference to C—C (sp^2) band in the carbon 1 s spectra at 284.5 eV. Measurements were made at a takeoff angle of 45° with respect to the sample surface plane. This resulted in a typical sampling depth of 3–6 nm (95 % of the signal originated from this depth or shallower). Quantification was done using instrumental relative sensitivity factors (RSFs) that account for the X-ray cross section and inelastic mean free path of the electrons.

2.2.7. Fourier transform infrared spectroscopy (FT-IR)

FT-IR was done in a Bruker vertex 80 spectrometer. Diffuse reflectance infrared Fourier transform spectroscopy (DRIFTS) was used to collect spectra for samples carbonized at 500 $^{\circ}\text{C}.$

3. Results and discussion

The TGA of the precursors before carbonization highlights the weight loss associated with the removal of heteroatoms before carbonization. Specifically, the analysis indicates that the resole precursor has the highest carbon yield compared to PVC, with the blend of resole and PVC yielding intermediate results (Supporting Information S1). We then calculated the carbon yields for all carbonized samples (Figs. 1a, b) for both atmospheric carbonization (APP) and autogenic pressure carbonization (AGP). APP_resole has a carbon yield of 72 %, slightly lower but

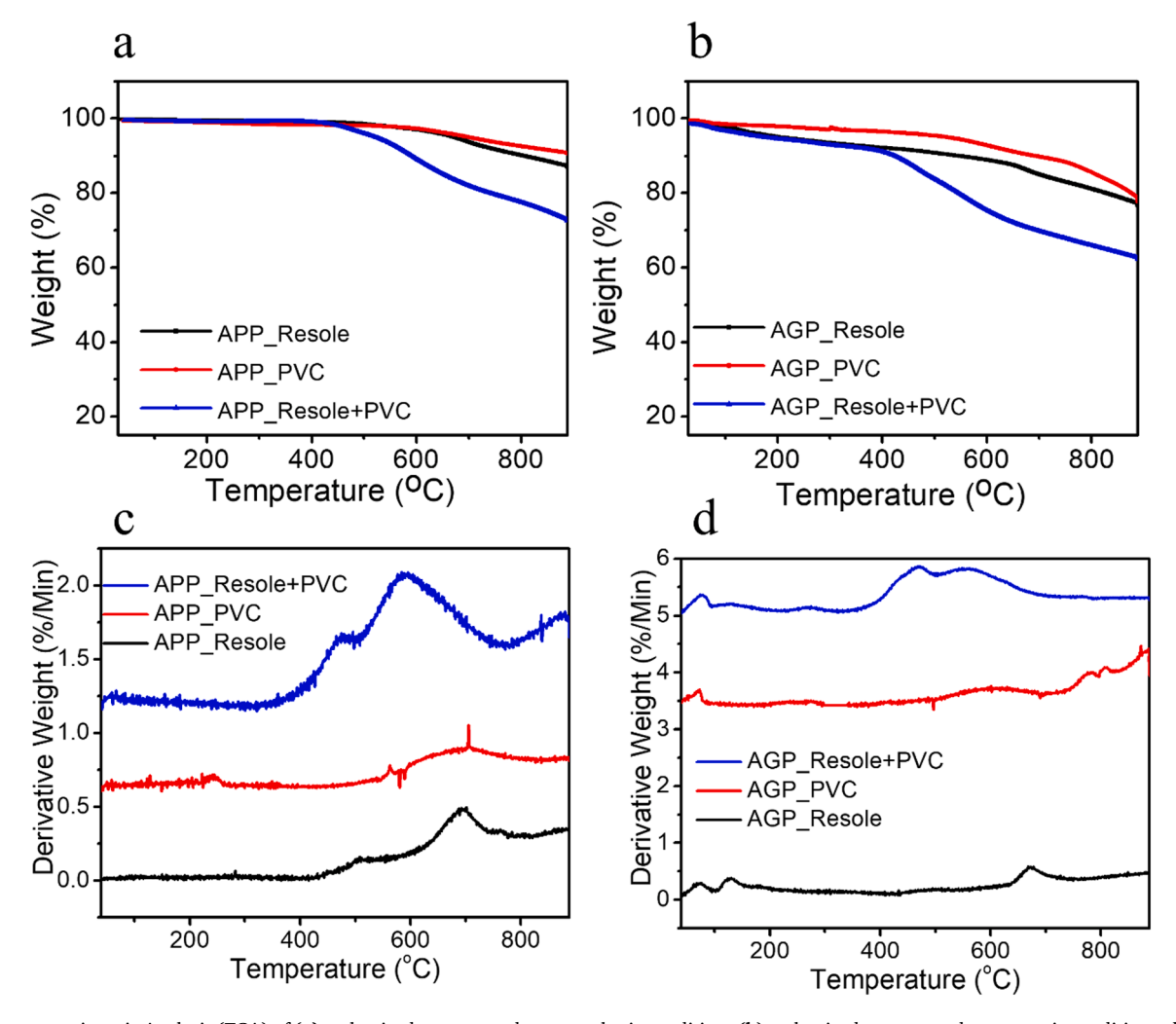


Fig. 1. Thermogravimetric Analysis (TGA) of (a) carbonized systems under atmospheric conditions (b) carbonized systems under autogenic conditions; derivative% weight curves of (c) samples carbonized under atmospheric conditions (d) samples carbonized under autogenic conditions.

comparable to the carbon yield of 79 % measured for AGP_resole. APP_PVC has a carbon yield of 90 % which is higher than the carbon yield measured for AGP_PVC (71 %). The higher degree of decomposition in AGP_PVC may be due to trapped volatiles in the matrix that were unable to escape from the closed reactor during carbonization. The same trend is observed in the mixture where the carbon content for APP_resole+PVC (88 %) is higher than AGP_resole+PVC (66 %). Generally, there is a low degree of decomposition observed across most samples

because a lot of volatiles have been lost during carbonization. The TGA derivative weights of the carbonized samples by both methods are plotted in Figs. 1c and d. For samples carbonized under APP conditions (Fig. 1c), APP_resole shows two decomposition peaks at approximately 515 °C and 700 °C. Similarly, APP_PVC has two decomposition peaks, one at 250 °C and a broad peak from 595 °C to 780 °C, and the blend (APP_resole+PVC) has two very pronounced decomposition peaks that occur at the same temperature as resole. The decomposition peak at 250

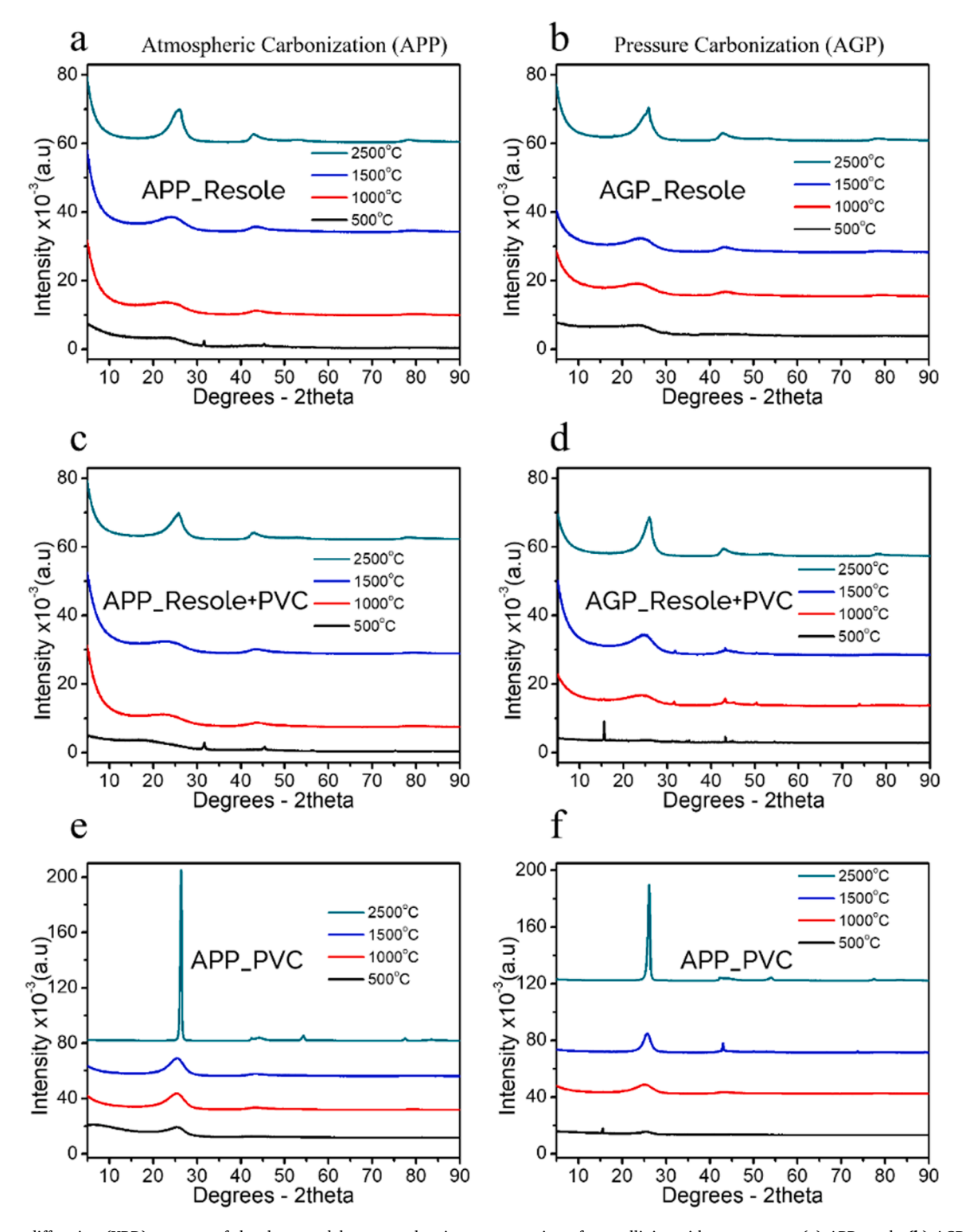


Fig. 2. X-ray diffraction (XRD) patterns of the three-model systems showing a progression of crystallinity with temperature (a) APP_resole (b) AGP_resole (c) APP_resole+PVC (d) AGP_resole+PVC (e) APP_PVC and (f) AGP_PVC.

°C in PVC is not seen in the blend. On the other hand, resole carbonized under autogenic condition (AGP_resole) shows three decomposition peaks at 75 °C, 115 °C, and 668 °C (Fig. 1d). AGP_PVC has multiple decomposition peaks above 600 °C while maintaining the broad peak from 595 °C to 780 °C observed in the derivative curve of APP_PVC. The blend, AGP_resole+PVC shows four decomposition peaks at 75 °C, 300 °C, 495 °C and 562 °C. For both carbonization methods, the rate with PVC and resole+PVC losses is much higher than pure resole resin. This is expected to lead to high porosity in PVC and resole+PVC as alluded to in previous work [20]. XPS and FT-IR analysis were conducted to compare the composition and structural difference between AGP and APP samples. Results from XPS (Supporting Information Table S1) show more chlorine on the pressure carbonized PVC and blend further agreeing with our possible hypothesis that pressure prevents volatiles and small molecules from escaping from the system. Also, the carbon content of pressure carbonization of resole leads to high carbon content as alluded to by other researchers. In addition, FT-IR of carbonized samples (Supporting Information S2) show that AGP resole has a prominent peak at 3050 cm⁻¹, corresponding to an aromatic CH vibration and a peak at 1700 cm⁻¹, representing C—O bond, suggesting a higher structural carbon content compared to APP resole. The most significant structural difference is observed in AGP resole+PVC with larger peaks at 3501 cm⁻¹ (-OH stretch) and 1609 cm⁻¹ (C = C) compared to the APP_resole+PVC, further supporting the hypothesis stated above.

Fig. 2. presents the X-ray diffraction (XRD) patterns of the threemodel systems showing a progression of crystallinity with temperature. Samples were heat treated at different temperatures: 1000 °C, 1500 °C, and 2500 °C. The heat treatment at 500 °C is the carbonization temperature used for all samples. APP_resole (Fig. 2a) has very broad peaks at 500 °C, 1000 °C, and 1500 °C; this represents the amorphous nature of the material. Even at high temperatures (2500 °C), resole is still an amorphous structure, typical of hard carbons. Although the d (002) peak and other high-angle peaks become more defined at 2500 $^{\circ}$ C, this does not signify any graphitization but rather the amorphous nature of resole even after high-temperature treatment. A similar observation can be seen in AGP_resole (Fig. 2b). There is no marked difference in the XRD spectra of the sample of resole carbonized under APP and AGP conditions. To summarize, resole is a non-graphitizable, hard carbon meaning it does not go through a mesophase fluid stage which allows for rearrangement and stacking of graphene sheets, rather it simply chars in place during carbonization. This is due to the formation of highly crosslinked and curved structures facilitated by the presence of oxygen functional groups. Even though there is an observed improved intensity/ growth of the d(002) peak of APP and AGP resole at 2500 °C, it is broad and does not resemble the very sharp and intense d(002) peak of pure graphite [18-23]. The improved intensity of the d(002) peak of resole can be attributed to small crystallites that formed at 2500 °C with no long-range order. Fig. 2c depicts the XRD spectra of the APP_resole+PVC mixture. There is no graphitization of the mixture even at an HTT of 2500 °C. Although the d(002) peak intensity increases as temperature increases, it is still very broad at 2500 °C[18-23]. A similar trend is illustrated in the XRD spectra of the AGP_resole+PVC mixture (Fig. 2d). Even though the mixture exhibited the same characteristic trend in carbon yield as PVC (soft carbon), from this result, it appears that the hard carbon, resole, dominates the structure after heat treatment and impedes the graphitization of the mixture. Fig. 2e shows the XRD spectra for APP_PVC graphitized at different temperatures. There is improved graphitization as temperature increases to 2500 °C evidenced by the increasing intensity and narrowing of the d(002) peak. There is also a clear definition of the peaks at higher degree angles. PVC is a graphitizing carbon therefore considered soft, non-porous, and passes through a fluid stage during carbonization. This fluidity phase is critical as it facilitates the molecular mobility of aromatic molecules resulting in intermolecular dehydrogenative polymerization reactions that create aromatic, lamellar disc-like molecules. A fluid phase is therefore one of the dominant requirements for graphitizing carbons[21]. The same

changes can be seen in AGP PVC in Fig. 2f.

Fig. 3. plots the XRD lattice parameters (d(002), La, and Lc) of the three-model system heat-treated at different temperatures. The d(002) is the typical primary measure for graphitization. As d(002) decreases, graphitic quality increases. In Fig. 3a. the d(002) trend for APP_resole is shown. As resole is heated and treated to higher temperatures, d(002) decreases. Despite the monotonic decrease in d(002) with increasing HTT, the d(002) value at 2500 °C is 0.346 nm, higher than that of pure graphite at 0.335 nm. This is consistent with the non-graphitizing characteristic of resole. The same trend can be seen in AGP_resole across the temperature series in Fig. 3b. At 2500 °C, the d(002) for AGP_resole is 0.346 nm. These results show that there is no significant difference between the resole carbonized under atmospheric or autogenic conditions. Fig. 3c. shows the d(002) plot for APP_PVC at different temperatures. The d(002) value decreases as temperature increases, reaching a value of 0.337 nm at 2500 °C, close to 0.335 nm for pure graphite [22-27]. PVC is a graphitizable carbon, and it passes through the mesophase stage during carbonization which allows for rearrangement and graphite sheet stacking at HTT. The same trend can be seen in AGP PVC in Fig. 3d where at 2500 °C, the d(002) is 0.339 nm. These results show that there is no significant difference between the graphitization of APP PVC and AGP PVC. The Lc values across the temperature series for systems carbonized under autogenic conditions are plotted in Fig. 3e. For all systems, there is an increase in Lc value at 2500 °C. The Lc value for the resole and the mixture (resole+PVC) is 3 nm. Thus, the non-graphitizing precursor dominates the quality and properties of the mixture after HTT. Meanwhile, the Lc value for PVC (14 nm) is significantly higher than that of resole and the mixture (resole+PVC). Fig. 3f shows the d(002) plot for AGP_resole+PVC as temperature increases. There is a decrease in d(002) as temperature increases. At 2500 $^{\circ}$ C, the d (002) value is 0.343 nm. The same values were obtained for the APP_resole+PVC mixture. These results show that there is no significant difference between APP_resole+PVC and AGP_resole+PVC after high-temperature treatment. From XRD analysis, measurements of the d (002) and Lc parameters show no significant differences in the samples carbonized under APP and AGP conditions.

Raman spectroscopy is another technique used to characterize the graphitic quality of samples. Fig. 4. depicts the Raman spectra of the 3model systems heat treated at 1500 °C and 2500 °C. Fig. 4a shows the Raman spectra for APP carbonized systems heat treated at 1500 °C. An equal intensity of the D and G bands can be observed in each sample, a hallmark of non-graphitic carbon. The d-band arises from a ringbreathing mode originating from disordered edges as a result of defects caused by the presence of sp³ carbons dangling from the edges, holes in the lattice, etc. [1,28,29]. This suggests that 1500 °C is a temperature too low to remove defects, enable sheet stacking, and thus improve graphitic quality. The same trend can be seen in the Raman spectra for the AGP carbonized systems heat treated at 1500 °C in Fig. 4b. There is no observable difference in the graphitic quality of the APP and AGP carbonized systems at 1500 °C. The Raman results agree with the XRD results in Fig. 3. Fig. 4c. shows the Raman spectra for APP carbonized systems graphitized at 2500 °C. In the spectra for APP_PVC, a very low d-band intensity, but a higher and narrower G-band intensity was observed, signaling a high degree of graphitization in PVC. The same trend can be seen in AGP_PVC at 2500 °C in Fig. 4d. Unlike the PVC sample, there is still the prominent presence of the D band in APP_resole and AGP_ resole after HTT at 2500 $^{\circ}\text{C}$ in Fig. 4c and 4d, respectively. This is because resole is a non-graphitizable carbon, it does not go through a fluid mesophase stage during carbonization which allows for initial stacking and rearrangement of graphene sheets, it simply forms chars. The spectra of APP_resole+PVC and AGP_resole+PVC in Fig. 4c and 4d, respectively, also show the presence of a prominent d-band. This signifies that the mixture is non-graphitizable. Although PVC is a soft carbon, these results indicate that when mixed with resole (a hard carbon), the resultant mixture takes the structure and graphitization behavior of the hard carbon. The La values calculated from Raman were

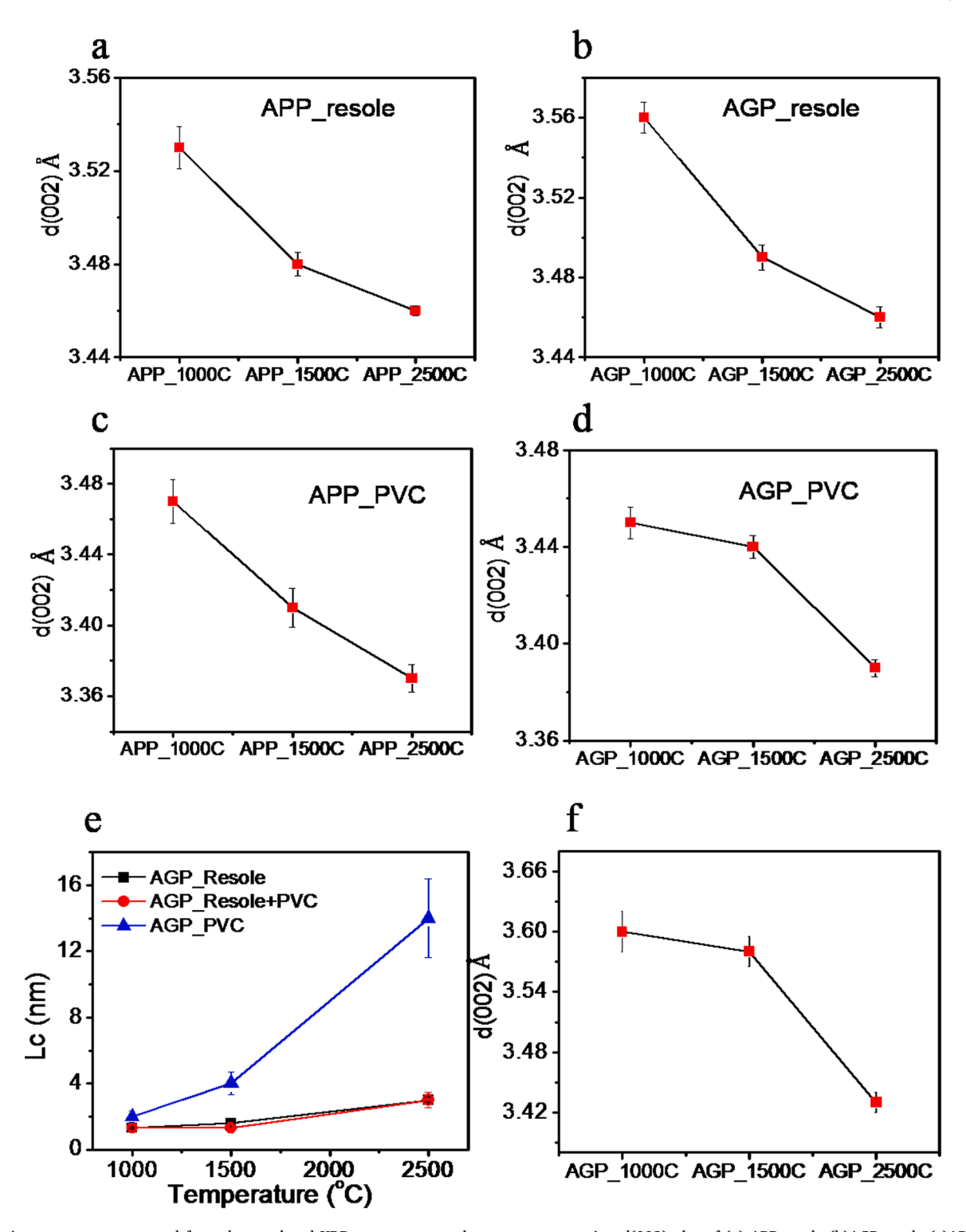


Fig. 3. Lattice parameters extracted from deconvoluted XRD spectra across the temperature series. d(002) plot of (a) APP_resole (b)AGP_resole (c)APP_PVC (d) AGP_PVC; (e) Lc plot of AGP systems; (f) d(002) plot of AGP_resole+PVC.

plotted (Fig. 4e). Resole and resole+PVC have low La values unlike PVC (graphitizing/soft carbon). There is an improvement in La values of the non-graphitizing carbons (resole and resole+PVC) carbonized under AGP conditions compared to when carbonized under APP conditions. The La value for AGP_resole is 4.5 nm compared to 3 nm for APP_resole. The same values were measured for AGP_ and APP_resole+PVC. However, the measured La values for PVC were 31 nm and 40 nm for APP_PVC and AGP_PVC, respectively. The I_D/I_G ratio is plotted in Fig. 4f.

AGP_resole and AGP_resole+PVC have a lower I_D/I_G ratio compared to APP_resole and APP_resole+PVC. PVC had the lowest I_D/I_G values from both methods, APP_PVC (0.11) and AGP_PVC (0.15) close to the values of graphite [30–33]. Pressure appears to not affect the improvement of graphitic quality for PVC (Fig. 4f).

A more in-depth Raman analysis reveals distinctions between the APP and AGP samples, as illustrated in Table 1. The initial column presents the intensity ratio of the D to G band (I_D/I_G), a metric reflecting

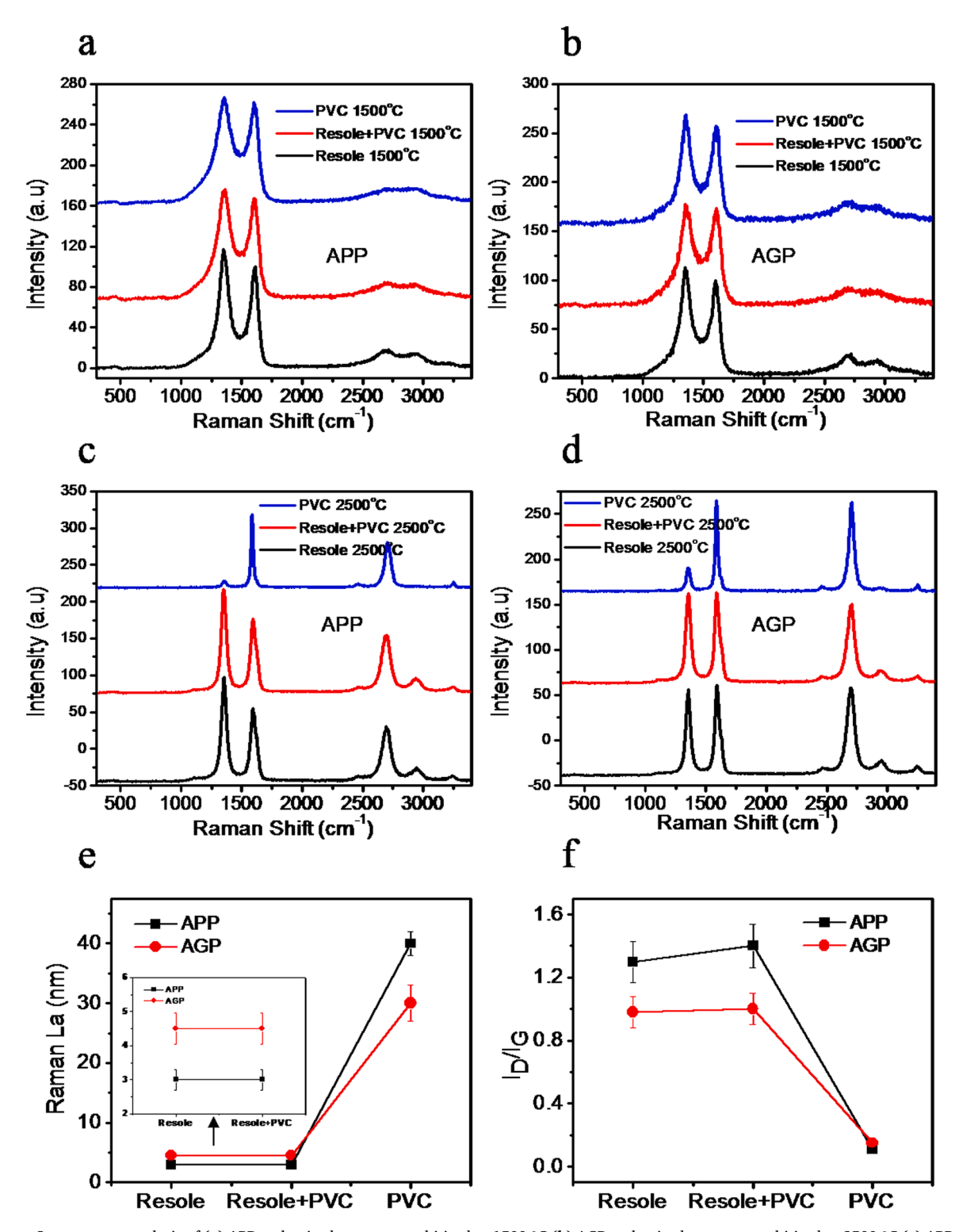


Fig. 4. Raman Spectroscopy analysis of (a) APP carbonized systems graphitized at 1500 °C (b) AGP carbonized systems graphitized at 2500 °C (c) APP carbonized systems graphitized at 2500 °C; Raman analysis of (e) crystallite length (La) and (f) I_D/I_G ratio comparison of APP and AGP samples at 2500 °C.

defect and disorder levels in samples. Decreasing I_D/I_G values correspond to heightened graphitic carbon content. APP_PVC and AGP_PVC exhibit comparable low I_D/I_G values of 0.11 and 0.15, respectively, indicative of low disorder and high graphitic quality. Conversely, the resole and resole+PVC mixture exhibit higher I_D/I_G ratios, suggesting increased defect levels and diminished crystalline quality. Notably, AGP_resole and AGP_resole+PVC display lower I_D/I_G ratios than their

APP counterparts, indicating fewer defects in the AGP samples. The subsequent columns detail the G-peak position, and the G-full width half-maximum (G-FWHM) provide clear evidence of the disparity in crystalline content between AGP and APP non-graphitic samples (resole and resole+PVC). The smaller, narrower G-FWHM signifies higher graphitic quality. AGP_resole and AGP_resole+PVC exhibit lower G-FWHM values than their APP counterparts, while APP_PVC and

Table 1Raman parameters for 2500C APP and AGP samples.

Samples	I_D/I_G	G-Peak position (cm- 1)	G FWHM	$I_{\rm 2D}/$ $I_{\rm G}$	2DFWHM/ GFWHM
APP_PVC	0.11	1585	22	0.36	2.47
AGP_PVC	0.15	1586	24	0.42	2.41
APP_Resole	1.44	1592	58	0.64	1.25
AGP_Resole	0.81	1593	48	0.83	1.49
APP_resole+PVC	1.55	1589	59	0.87	1.26
$AGP_resole + PVC$	1.1	1590	44	0.98	1.55

AGP PVC show comparable G-FWHM values.

Further analysis of Raman parameters, including the ratio of the 2D to G band ($I_{\rm 2D}/I_{\rm G}$), underscores improved graphitic layers in AGP samples, as they exhibit higher $I_{\rm 2D}/I_{\rm G}$ values than their APP counterparts. This trend is also observed in the full-width half-maximum (FWHM) ratio of the 2D to G band in the last column, with higher values for AGP samples compared to their APP counterparts (except for PVC, which shows comparable values). These findings suggest lower defects, and enhanced crystalline content in AGP samples, particularly in the hard carbon samples, AGP_resole and AGP_resole+PVC. It appears that carbonization under pressure can influence the formation of larger crystallites and improve the overall structure.

Scanning electron microscopy (SEM) was used to study the

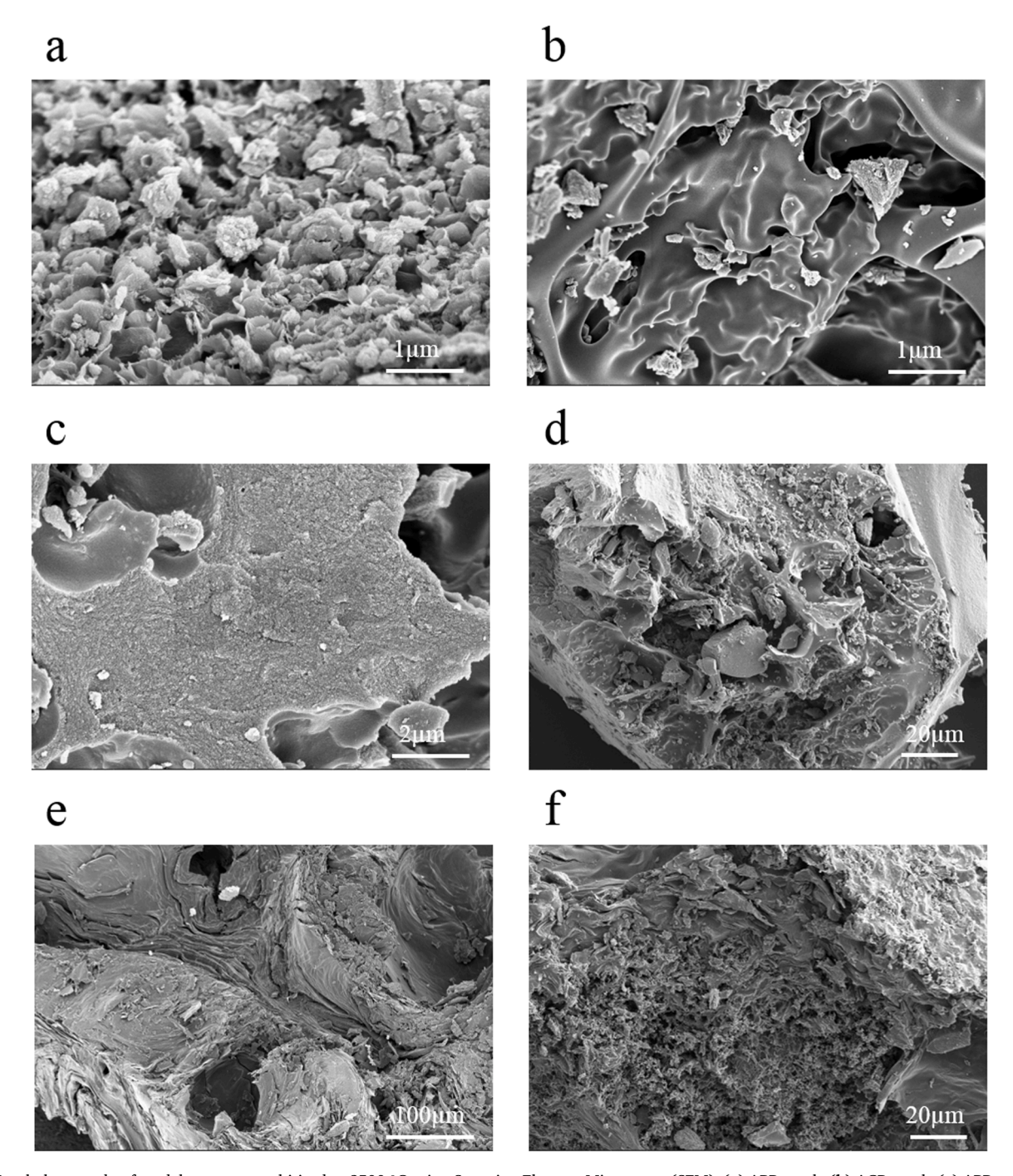


Fig. 5. Morphology study of model systems graphitized at 2500 °C using Scanning Electron Microscopy (SEM). (a) APP_resole (b) AGP_resole (c) APP_resole+PVC (d) AGP_resole+PVC (e)APP_PVC and (f) AGP_PVC.

morphology of heat-treated samples at 2500 °C. Figs. 5a and b show SEM micrographs of APP_resole and AGP_resole, respectively. There is a high density of small aggregates of carbons with no observation of orderliness in APP_resole. AGP_resole shows flakes and aggregates appearing in wavy-like morphology. This morphology could be due to the nongraphitizing nature of phenolic resin which forms disordered structures even after HTT at 2500 °C. Figs. 5c and d show SEM micrographs of the APP resole+PVC and AGP resole+PVC, respectively. A lack of a layered structure is observed in both images. Samples appear as aggregated carbons and large flakes with no orientation or layers. However, the SEM images reveal that the blend carbonized under autogenic pressure conditions (AGP_resole+PVC) exhibits significantly higher porosity compared to its APP counterpart (Supporting Information S3). This increased porosity in the AGP_resole+PVC sample suggests that the pressurized carbonization process effectively enhances the formation of porous structures, which could be beneficial for applications requiring high surface area and improved material interaction, such as in battery electrodes or catalytic supports. Conversely, the SEM images of APP_PVC (Figs. 5e) and AGP_PVC (Figs. 5f) show a more pronounced

compact multilamellar structure. AGP_PVC also has some sections of roughness arising from aggregates (non-homogeneity). This evidence supports results from Raman where a low d-band intensity is seen in the spectra. XRD and Raman support graphitization of the PVC sample.

Transmission electron microscopy (TEM) was used to investigate the nanostructure distinctions between the graphitized AGP and APP samples. Corresponding selected area electron diffraction (SAED) patterns were collected to provide insights into their crystallinity, emphasizing subtleties that may arise from the differing carbonization methods. The nanostructure of APP_PVC (depicted in Fig. 6a) reveals sheet stacking without wrinkles or curvature, indicative of a graphitizing carbon. The accompanying SAED pattern (Fig. 6b) forms a polycrystalline ring, representing periodic crystallites along grain boundaries. This nanostructure and the supporting SAED pattern align with XRD and Raman results, confirming that PVC manifests as a graphitic carbon at 2500 °C. Similarly, AGP_PVC (Fig. 6c) exhibits sheet stacking and the presence of lattice fringes, signifying long-range order in the material. The corresponding SAED pattern (Fig. 6d) is also polycrystalline with a sharp and defined crystallite orientation similar to APP_PVC.

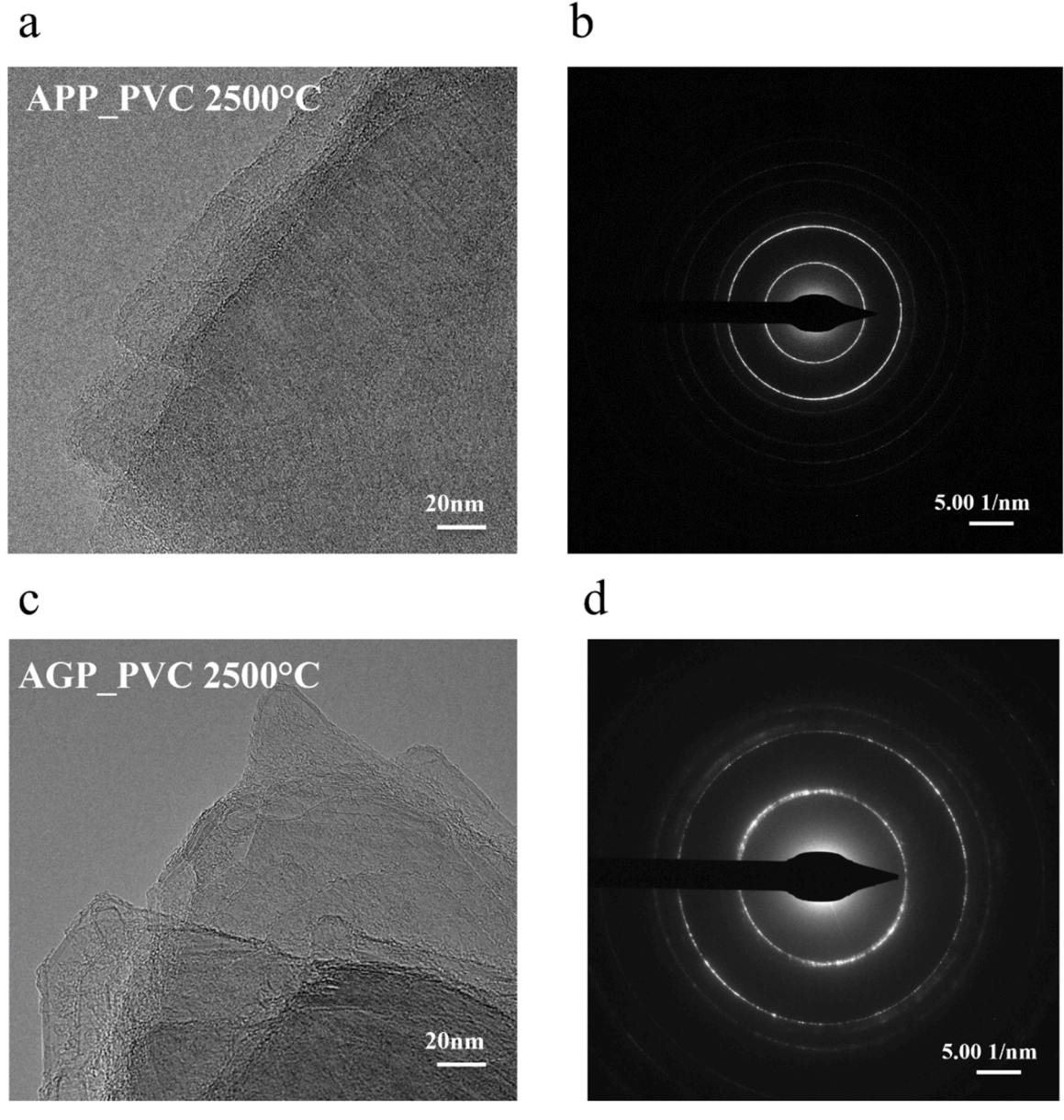


Fig. 6. TEM and SAED images of APP_PVC (a,b) and AGP_PVC (c,d).

In contrast to the graphitic and well-ordered nanostructure observed in PVC, APP_resole (depicted in Fig. 7a) unveils a fullerenic curved nanostructure. The corresponding selected area electron diffraction (SAED) pattern (Fig. 7b) appears amorphous, characterized by halo rings, thus confirming the non-graphitic nature of resole — an observation in agreement with XRD and Raman analyses. Similarly, AGP_resole exhibits non-graphitic characteristics, with sporadic areas featuring lattice fringes (Fig. 7c). The resulting SAED pattern indicates a blend of amorphous and polycrystalline elements, suggesting the presence of crystallites. While this doesn't signify long-range order in the AGP_resole sample, it does imply the development of larger crystallites in the AGP carbonized sample.

The characteristic of a non-graphitizing nanostructure persists in the resole+PVC mixture. In APP_resole+PVC (Fig. 8a), a multitude of curved lamellae is evident, and the corresponding selected area electron diffraction (SAED) pattern (Fig. 8b) showcases amorphous halo rings. Similarly, the AGP mixture exhibits a comparable nanostructure to its APP counterpart (Fig. 8c), albeit with instances of short-stack lamellae

highlighted in the red box. This is further elucidated by the SAED pattern (Fig. 8d), which reveals a combination of amorphous and polycrystalline patterns—consistent with the trends observed in the materials. These observations underscore the formation of larger crystallites in the AGP carbonized samples which was also confirmed by Raman analysis. Pressure carbonization improves the formation of larger crystallites in the non-graphitizing precursors and can therefore influence their various industry applications such as for energy storage where materials with larger crystallite size (La) have been shown to lead to improved capacity.

5. Conclusion

This work showed improved graphitization/graphitic quality in non-graphitizing precursors as a consequence of pressurized carbonization. XRD crystalline peak at 26.2° is much sharper in autogenic pressure carbonization for both resole and resole+PVC signifying higher crystallinity in the hard carbons. The crystallite parameter, specifically

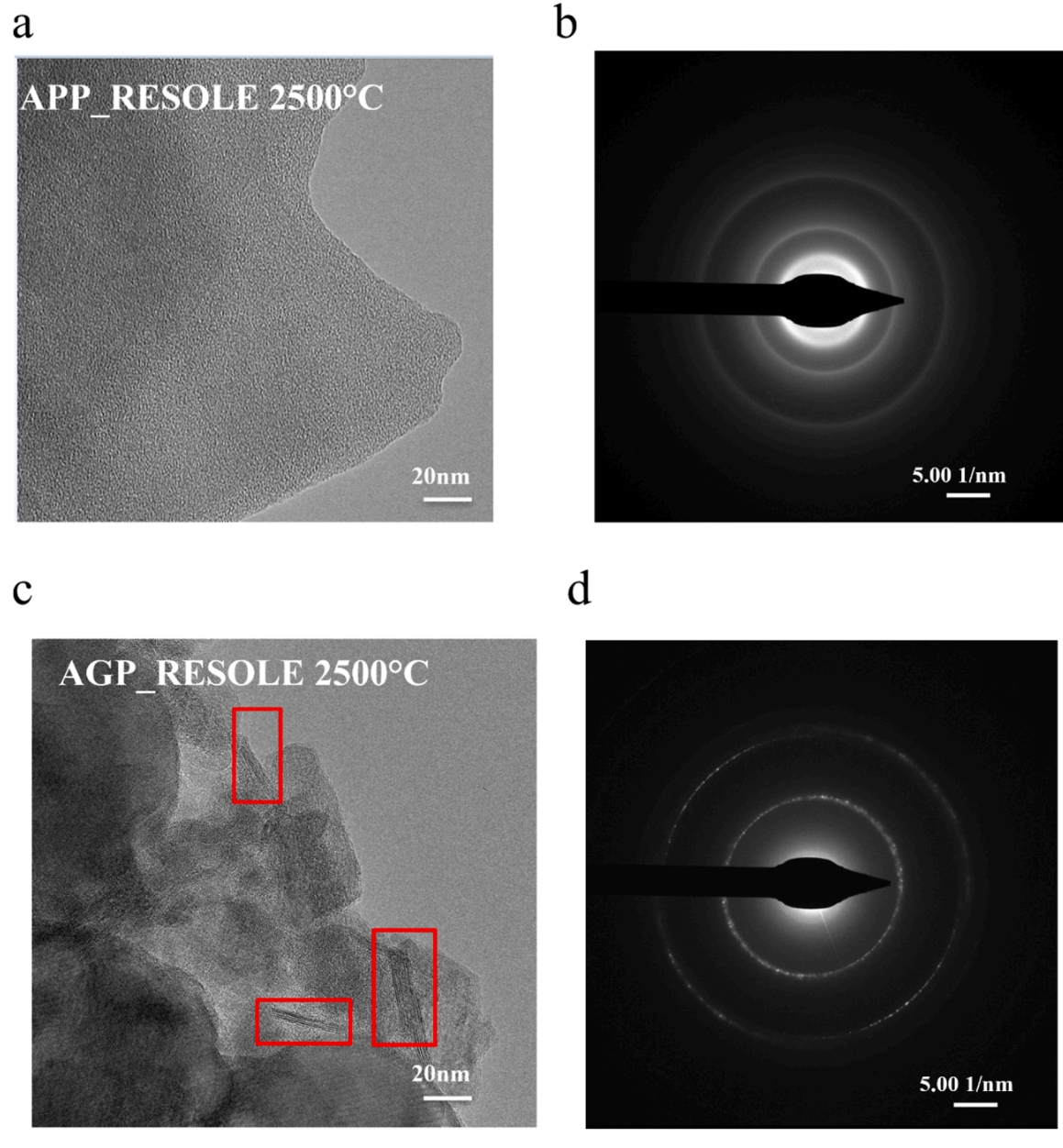


Fig. 7. TEM and SAED images of APP_resole (a,b) and AGP_resole (c,d).

a b

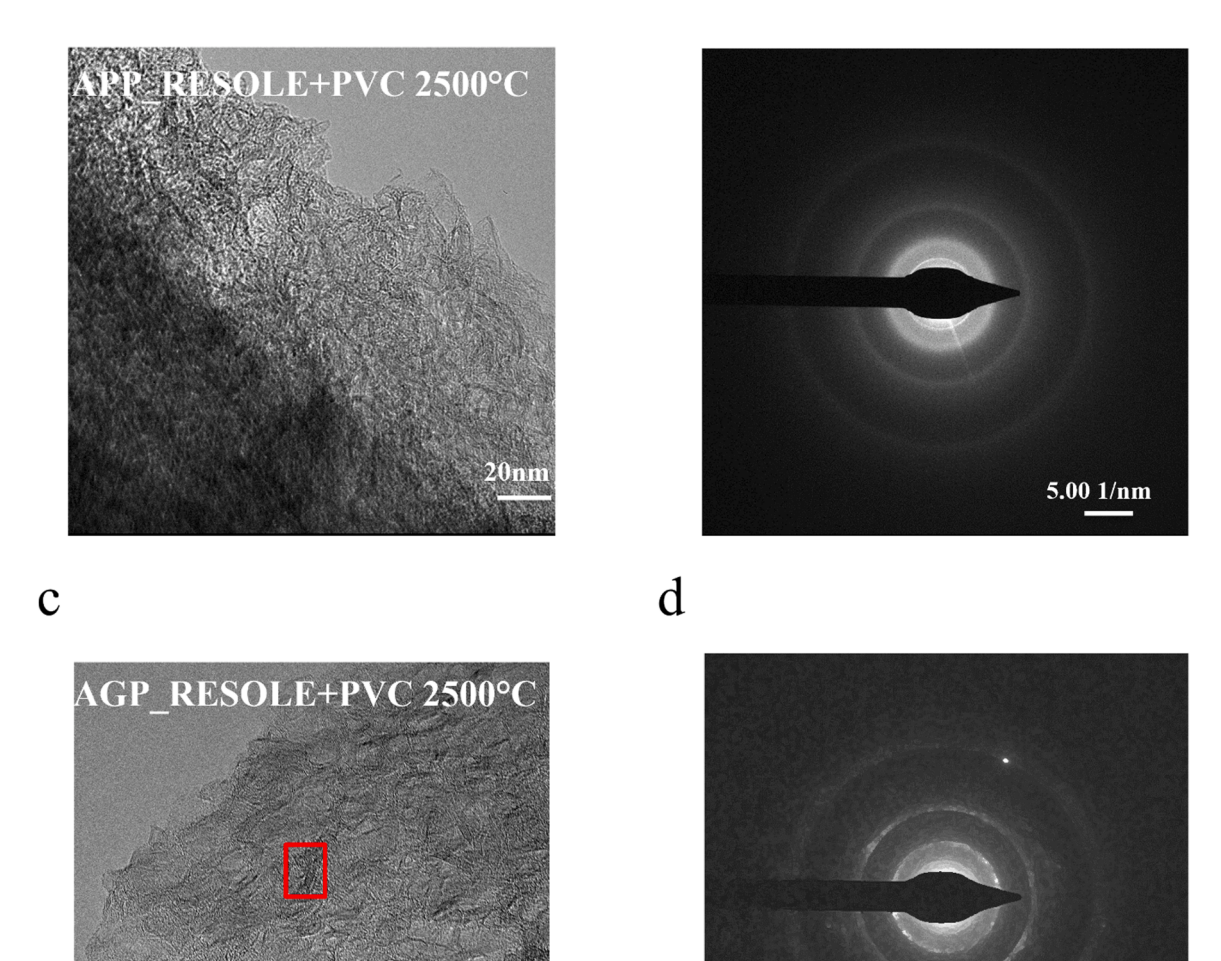


Fig. 8. TEM and SAED images of APP_resole+PVC (a,b) and AGP_resole+PVC (c,d).

20nm

crystallite size, La, increased as measured by Raman analysis. Additional Raman analysis in the terms of I_D/I_G ratio, G-FWHM, and ratios of intensity and FWHM of the 2D to G band signified lesser disorder and improved crystalline content in the non-graphitizing precursors, AGP resole and AGP resole+PVC. Furthermore, transmission electron microscope (TEM) shows areas of lattice fringe growth in the nanostructure and brighter larger crystallites in the SAED patterns in AGP_resole and AGP_resole+PVC. This improvement in crystallite size can be attributed to the pressurized condition of carbonization where volatiles and small molecules are not allowed to escape and hence can attach to edge sites facilitating crystallite size growth (lateral extent). For the soft carbon precursor (PVC), the graphitization does not depend on carbonization pressure. This work is important due to the growing need to identify procedures for hard carbon precursors into synthetic graphitic carbons. We have shown that carbonization pressure can improve the crystallinity of hard carbons. Even though fully graphitic materials were not achieved, the results suggest that with higher pressure during carbonization, this may be possible. A follow-up study could explore the impact of deliberately applying range of fixed external pressure during carbonization. This promising progress may lead to

alternative precursors for synthetic graphite production.

CRediT authorship contribution statement

Sandra Ike: Conceptualization, Data curation, Formal analysis, Investigation, Methodology, Validation, Visualization, Writing – original draft, Writing – review & editing. **Randy Vander Wal:** Methodology, Supervision, Validation, Writing – review & editing.

5.00 1/nm

Declaration of competing interest

The authors declare that they have no known competing financial interests or personal relationships that could have appeared to influence the work reported in this paper.

Data availability

No data was used for the research described in the article.

Acknowledgement

This material is based upon work supported by the National Science Foundation under Grant No. (2306042). Acknowledgment is also made to the donors of the American Chemical Society Petroleum Research Fund for support of this research.

Supplementary materials

Supplementary material associated with this article can be found, in the online version, at doi:10.1016/j.cartre.2024.100382.

References

- [1] T. Aziz, D. Das, J.J. Bora, A. Namdeo, Production and applications of biochar, Prod. Appl. Biochar (2022) 263–286.
- [2] M.J. Gonzalez-Cimas, J.W. Patrick, A. Walker, Influence of pitch additions on coal carbonization. Coke strength and structural properties, Fuel 66 (1987) 1019–1023, https://doi.org/10.1016/0016-2361(87)90294-8.
- [3] Y. Shen, A review on hydrothermal carbonization of biomass and plastic wastes to energy products, Biomass Bioenergy 134 (2020) 105479, https://doi.org/10.1016/ i.biombioe.2020.105479.
- [4] I.C. Lewis, Chemistry of carbonization, Carbon N. Y. 20 (1982) 519–529, https://doi.org/10.1016/0008-6223(82)90089-6.
- [5] M. Inagaki, F. Kang, M. Toyoda, H. Konno, Carbonization under pressure, Adv. Mater. Sci. Eng. Carbon. 4 (2014) 67–85, https://doi.org/10.1016/b978-0-12-407789-8.00004-1.
- [6] P. Rousset, C. Figueiredo, M. De Souza, W. Quirino, Pressure effect on the quality of eucalyptus wood charcoal for the steel industry: a statistical analysis approach, Fuel Process. Technol. 92 (2011) 1890–1897, https://doi.org/10.1016/j. fuproc.2011.05.005.
- [7] M.A. Trofimovich, A.A. Galiguzov, A.P. Malakho, V.V. Avdeev, Effect of pressure on carbonization of coal tar pitch of different composition, Refract. Ind. Ceram. 56 (2015) 286–291, https://doi.org/10.1007/s11148-015-9832-2.
- [8] M. Inagaki, K.C. Park, M. Endo, Carbonization under pressure, New Carbon Mater 25 (2010) 409–420, https://doi.org/10.1016/S1872-5805(09)60042-1.
- [9] D.M. Manohar, V. Raju, Effect of pressure and temperature on properties of carboncarbon composites prepared from renewable material, Int. Conf. Control. Comput. Commun. Mater. (2016) 1–5.
- [10] J.R. Kershaw, P.J. Smart, Extraction of coal-tar pitch and the effect on carbonization, Carbon N. Y. 32 (1994) 85–92, https://doi.org/10.1016/0008-6223 (94)90012-4.
- [11] J. González-Arias, M.E. Sánchez, J. Cara-Jiménez, F.M. Baena-Moreno, Z. Zhang, Hydrothermal carbonization of biomass and waste: a review, Environ. Chem. Lett. 20 (2022) 211–221, https://doi.org/10.1007/s10311-021-01311-x.
- [12] J. Ayache, A. Oberlin, M. Inagaki, Mechanism of carbonization under pressure, part I: influence of aromaticity (polyethylene and anthracene), Carbon N. Y. 28 (1990) 337–351, https://doi.org/10.1016/0008-6223(90)90007-L.
- [13] T. Hosomura, H. Okamoto, Effects of pressure carbonization in the CC composite process, Mater. Sci. Eng. A. 143 (1991) 223–229, https://doi.org/10.1016/0921-5003(01)00741-5
- [14] M. Inagaki, K. Kuroda, M. Sakai, E. Yasuda, S. Kimura, Carbonization of fractionated pitches under pressure, Carbon N. Y. 22 (1984) 335–339, https://doi. org/10.1016/0008-6223(84)90003-4.

- [15] S.H. Kamiya Kan-ichi, Michio Inagaki, Effect of pressure on graphitization of carbon. VI. Normal pressure heat treatment of soft carbon pre-heat-treated under high pressure, Bull. Chem. Soc. Japan. 42 (1969) 1425–1428.
- [16] H. Okamoto, T. Hosomura, K. Kosaka, Effect of pressure carbonization in carbon/carbon composite process(II), MRS Online Proc. Libr. (1991) 99–104. https://www.unhcr.org/publications/manuals/4d9352319/unhcr-protection-training-manual-european-border-entry-officials-2-legal.html?query=excom1989.
- [17] J.P. Abrahamson, A. Jain, A.C.T. van Duin, R.L. Vander Wal, Carbon structure and resulting graphitizability upon oxygen evolution, Carbon N. Y. 135 (2018) 171–179, https://doi.org/10.1016/j.carbon.2018.04.055.
- [18] S. Dyjak, I. Wyrębska, A. Błachowski, W. Kaszuwara, K. Sobczak, M. Polański, M. Gratzke, W. Kiciński, The role of heteroatoms in iron-assisted graphitization of hard carbons derived from synthetic polymers: the special case of sulfur-doping, Carbon N. Y. 218 (2024), https://doi.org/10.1016/j.carbon.2023.118717.
- [19] C. Fan, R. Zhang, X. Luo, Z. Hu, W. Zhou, W. Zhang, J. Liu, J. Liu, Epoxy phenol novolac resin: a novel precursor to construct high-performance hard carbon anode toward enhanced sodium-ion batteries, Carbon N. Y. 205 (2023) 353–364, https:// doi.org/10.1016/j.carbon.2023.01.048.
- [20] D. Dacey, J. Cadenhead, The formation of carbon from polyvinylidene chloride, in: Proc. Fourth Conf. Carbon, 1960, pp. 315–319.
- [21] R.E. Franklin, Crystallite growth in graphitizing and non-graphitizing carbons, Proc. R. Soc. London. Ser. A. Math. Phys. Sci. 209 (1951) 196–218, https://doi. org/10.1098/rspa.1951.0197.
- [22] L. Alcaraz, D. Carlos, Obtaining and characterization of highly crystalline recycled graphites from different types of spent batteries, Materials (Basel) (2022) 3246.
- [23] J.U. Hwang, W. Jun, A. Ji, S. Im, J.D. Lee, Properties of synthetic graphite from boric acid - added pitch: performance as anode in lithium-ion batteries, SN Appl. Sci. (2021), https://doi.org/10.1007/s42452-021-04566-9.
- [24] C. Bao, Q. Zeng, F. Li, L. Shi, W. Wu, L. Yang, Y. Chen, H. Liu, Effect of boron doping on the interlayer spacing of graphite, Materials (Basel) (2022) 4203.
- [25] A. Vlahov, XRD graphitization degrees: a review of the published data and new calculations, correlations, and applications, Geol. Babcanica. 50 (2021) 11–35.
- [26] T. Qiu, J. Yang, X. Bai, Y. Wang, with hierarchical pores from lignite by one-step, RSC Adv (2019) 12737–12746, https://doi.org/10.1039/c9ra00343f.
- [27] A. You, M.A.Y. Be, I. In, Synthesis of few-layer graphene by direct exfoliation of graphite and a Raman spectroscopic study, AIP Adv (2014) 027116, https://doi. org/10.1063/1.4866595.
- [28] A. Beda, P. Taberna, P. Simon, C.M. Ghimbeu, A. Beda, P. Taberna, P. Simon, C. Matei, G. Hard, Hard carbons derived from green phenolic resins for Na-ion batteries, Carbon N. Y. (2019) 248–257.
- [29] A. Oberlin, Carbonization, Carbon N.Y. 22 (1984) 521–541.
- [30] A. Inam, R. Brydson, D.V. Edmonds, Materials Characterization Raman spectroscopy study of the crystallinity of graphite formed in an experimental freemachining steel, Mater. Charact. 163 (2020) 110264, https://doi.org/10.1016/j. matchar.2020.110264.
- [31] M.A. Pimenta, G. Dresselhaus, M.S. Dresselhaus, L.G. Canc, Studying disorder in graphite-based systems by raman spectroscopy w, Phys. Chem. Chem. Phys. (2007) 1276–1291, https://doi.org/10.1039/b613962k.
- [32] S.S. Bukalov, L.A. Leites, R.R. Aysin, Laser raman micro-spectroscopy as an effective non-destructive method of detection and identification of various sp 2 carbon modifications in industry and in nature **, Adv. Mater. Lett. 10 (2019) 550–562, https://doi.org/10.5185/amlett.2019.2268.
- [33] L. Bokobza, J. Bruneel, M. Couzi, Raman spectra of carbon-based materials (from Graphite to Carbon Black) and of some silicone composites, C. (2015) 77–94. doi:10.3390/c1010077.